doi: 10.5028/jatm.2012.04043112

Propeller-induced Effects on the Aerodynamics of a Small Unmanned Aerial Vehicle

Adnan Maqsood*[1], Foong Herng Huei[2], Tiauw Hiong Go[2]
[1]National University of Sciences and Technology – Islamabad – Pakistan
[2]Nanyang Technological University – Singapore

Abstract: *The present paper has discussed investigations about the propeller slipstream effects on the aerodynamics of a generic unmanned air vehicle platform in the wind tunnel for a broad advance ratio range. The propeller-induced effects for small unmanned air vehicles are more significantly pronounced than general aviation aircraft, because of their high propeller-diameter-to-wing-span-ratio. The stall angle of attack of the small unmanned air vehicle is generally delayed under slipstream effects. The study evaluated the shift in stall angle of attack as a function of propeller-diameter-to-wing-span and advance ratios of the propeller. The aerodynamics of the unmanned air vehicle platform is estimated through wind-tunnel experiments. The study reported in this paper is part of an effort to develop the framework for the analysis of propeller-wing interaction for small/micro unmanned air vehicles at an early design stage. Specifically, the slipstream effects on the aerodynamics of a generic small unmanned air vehicle are studied in the wind tunnel for the shift in the aircraft stall angle of attack. The lift-curve slope of the aircraft is independent from the variation of advance ratio. The stall characteristics show strong dependence on the advance ratio. Therefore, the relationship is modeled accurately using inverse-quadratic relationship. This empirical trend of the stall behavior with advance ratio can be useful in the analysis and simulation of the resulting flight and estimation of performance envelopes.*

Keywords: *Unmanned air vehicle, Propeller interaction, Powered testing, Wind-tunnel testing.*

INTRODUCTION

The demand for customized small-scale unmanned air vehicles (UAV) to execute different mission profiles has increased over the years. Significant efforts are underway to enhance the flight envelope of such UAV. One of them is the incorporation of hover capability in fixed-wing aircraft designs. Readers may find the associated development of such platforms in Taylor and Thomas Cord (2003), Green and Oh (2005), Frank et al. (2007), Stone et al. (2008), Maqsood and Go (2010). During hover/slow forward flight phase, the aircraft flies at high power, low velocity flight condition, which corresponds to low advance ratio of the propeller.

For the fixed-wing forward flight, the aircraft flies at high advance ratios (low power and high velocity). The flight envelope of hover capable fixed-wing designs can generally span from zero to substantially high advance ratios. In an experiment with limited advance ratio range from 1.15 to 2.48 and free-stream velocity of 35 m/s, Witkowski *et al.* (1989a, b) have observed that the aerodynamic behavior of the aircraft significantly changes with the change in advance ratio. This observation, however, is not well-followed by other researchers. Only very few studies adequately address the prop-stream effects over the broader range of advance ratios and, thus, such topic may still be considered as a missing link in literature. Few studies (Stone, 2002) emphasize on the importance of prop-wing interaction at zero/low translational velocities (low advance ratio). The work carried out by Stone (2002) comprises numerical modeling and is based on superimposition of prop-stream in numerical panel methods.

The prop-stream effects for the small/mini UAV have another pronounced implication. For a large-scale aircraft, the propeller-diameter-to-wing-span ratio (*d/b*) is relatively small, generally ranging from 0.2 to 0.3. For small/micro UAVs, however, the it can vary from 0.4 to 1.0, indicating that the diameter of the propeller is often comparable to the wingspan of the UAVs. As a result, the flow over the wings for

Received: 04/06/12 Accepted: 08/08/12
*author for correspondence: adnan@rcms.nust.edu.pk
Research Center for Modeling and Simulation, National University of Sciences and Technology, H-12, Islamabad, Pakistan

such vehicles is heavily influenced by the propeller-induced flows. Clearly, for higher *d/b* values, the power effect is more significant to the overall aerodynamic behavior of the aircraft.

One of the important aerodynamic behavior changes with power effects is on the lift characteristics with the angle of attack. Witkowski *et al.* (1989a) observed the lift-curve slope decreases as the advance ratio of the propeller increased. The percentage decrease of the lift slope is documented as 3.5% for advance ratio of 1.15 and *d/b* in the range of 0.16 to 0.3. The power effects on the stall characteristics are also found to be significant. Ralston and Hultberg (2010) reported that for a general aviation aircraft, the stall angle is significantly delayed/diminished as the advance ratio of the propeller is decreased (high power/low speed flight). Null *et al.* (2005) also observed the change in the stall angle of the aircraft with that in advance ratio, but did not quantify the phenomenon in their experimental investigations. It seems that a quantification of power effects on stall angle of attack is necessary for flight-dynamic simulations as part of the aircraft design and development.

The study reported in this paper is part of an effort to develop the framework for the analysis of propeller-wing interaction for small/micro UAVs at an early design stage. Specifically, the slipstream effects on the aerodynamics of a hover-capable generic small UAV are studied in the wind-tunnel for a broad advance ratio range. The propeller effects on the lift curve slope and stall angle of attack pattern are also studied. The present work also provides directions for further investigations involving various design parameters.

EXPERIMENTAL SETUP AND TESTING

The aircraft that is shown in Fig. 1 is the same platform used for the transition flight analysis (Maqsood and Go, 2010). It has a standard tractor type propulsion system with *d/b* of 0.5. This allows propeller-induced flows to be generated over a large portion of the wings. The small UAV is specifically designed to maneuver in tight spaces and can hover over the target area of interest. The span and length of the aircraft are 0.5 m. The airfoil for the rectangular-wing and horizontal tail is NACA 0012. The wind-tunnel model is fabricated from Aluminum T6061 at Nanyang Technological University (NTU).

The experiment was carried out at a low-turbulence, closed-circuit wind-tunnel at Nanyang Technological University (NTU). The operating speed of the wind-tunnel ranges from 6 to 90 m/s. Its high contraction ratio of 9 with a rectangular inlet contraction cone as well as the installment of three anti-turbulence screens with different meshes are specifically designed for achieving low-turbulence intensities. It is rated at a maximum of 0.1% turbulence level in axial direction. The test section used was 2-m-long with a rectangular cross-sectional area of 0.78 by 0.72 m. The model was mounted inside the wind-tunnel with a sting support. A six-component internal balance was used to measure lift, drag, and pitching moments. The data are recorded for 15 seconds for each scenario with a sampling rate of 47 Hz. Therefore, each datum is a time-averaged value taken over 700 samples approximately.

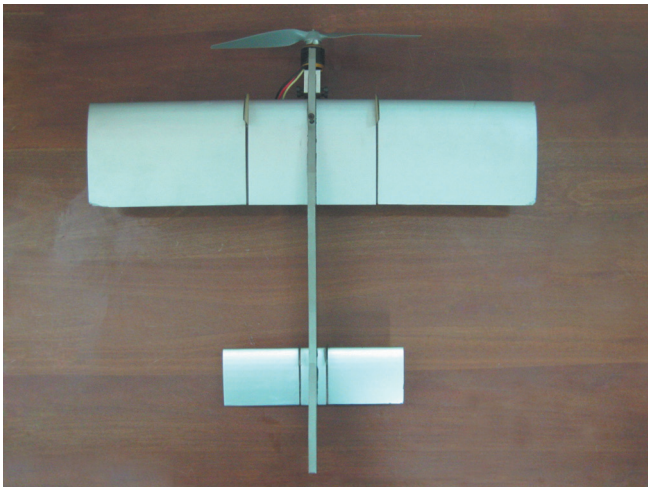

Figure 1. View of the unmanned air vehicle with motor installed.

The aerodynamic coefficients presented in this work have all been corrected for wind-tunnel blockage effects (solid blockage, wake blockage, and streamline curvature), according to the techniques presented by Barlow *et al.* (1999). The magnitude of the blockage effects increases with the increase in the angle of attack. The magnitude of blockage corrections for most of the scenarios is found to be less than 15%.

The propeller used in the experiment was a 10“ x 5″ thin two-bladed propeller driven by a brushless AXI 2217/16 electric motor through the Tahmazo® Pro C Max 1812-3S electronic speed controller (ESC). The control signal from a personal computer (PC) to the ESC was sent through the Pololu® Serial 8 Servo Controller interface. The control signal from the PC can vary from 0 to 255 bits. The revolution rate of the propeller was calibrated against the control signal. To power this setup, a GW Instek PSH 3630A ground-based direct current (DC) source was used. The maximum power supplied to the motor was 110 W (11 V, 10 A) at any instant during testing. The schematic of the propulsion system setup for the experiment is shown in Fig. 2.

The relationship of the propeller driven propulsion system is developed from the velocity of the aircraft, the blade-pitch angle of the propeller, and the advance ratio. For the fixed-

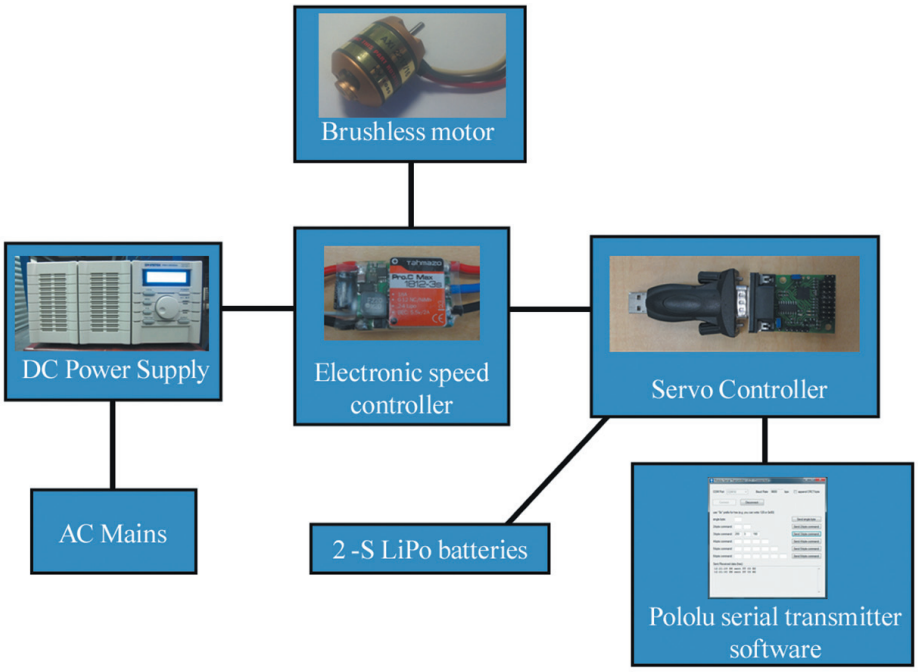

Figure 2. Schematic of the propulsion system and its controller.

pitch propeller, the advance ratio is the primary entity to describe the relationship. The advance ratio (J) of the propeller is defined as the ratio between the distance the propeller advances forward during one revolution and the diameter of the propeller. Mathematically, it can be expressed as in Eq. 1:

$$J = \frac{V_\infty}{N \times D} \tag{1}$$

where

V_∞ : is the true airspeed of the aircraft in m/s,

N: is the number of revolutions per second of the propeller, and

D: is the diameter of the propeller.

The advance ratio (Eq. 1) can be varied either by changing the free-stream velocity in the wind-tunnel or the revolution rate of the propeller. Both approaches have certain limitations. The change in the free-stream velocity causes variation in the Reynolds number of the experimental data, whose effect increases with the addition in the velocity envelope of the testing. For small UAV applications, the velocity envelope is small and, therefore, the effects are generally not significant. However, appropriate checks are required to remove the effect of Reynolds number in the experimental data. On the other hand, the increase in the RPM of the propeller can eventually lead the propeller tip to reach sonic speeds. In this work, data were collected at constant 6,070 RPM, which correspond to 100% throttle setting, and several velocities ranged from 7 to 22 m/s. Generally, the aircraft flies at lower throttle settings, but the presented series of tests were conducted at maximum throttle setting to delineate the maximum effects of propeller-induced flows. The relationship between the advance ratio of fixed-pitch propeller and free-stream velocity is of linear behavior (Ralston and Hultberg, 2010), and this is also obvious from Eq. 1.

The unpowered lift coefficient is plotted against the angle of attack for various Reynolds numbers in Fig. 3. It can be observed that the lift-curve slope is practically independent of Reynolds number. Moreover, the stall angle of attack is constant across the complete Reynolds number variation from

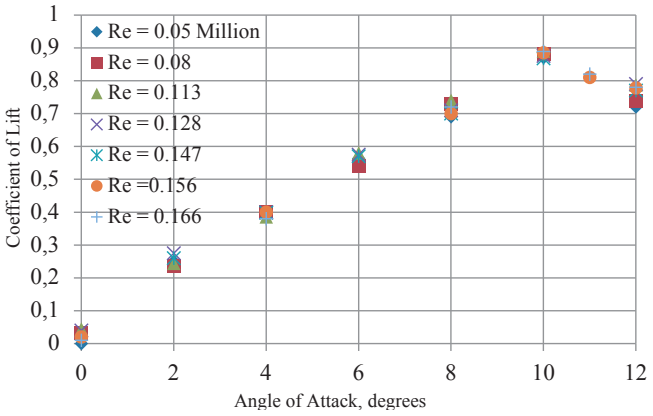

Figure 3. Unpowered lift coefficient for the test unpowered Reynolds number range.

0.05 to 0.16 million. It can be inferred that the velocity variation by itself is small enough to introduce any effect of Reynolds number on lift curve slope and stall angle of the aircraft.

Then, the mapping of thrust against the advance ratio was carried out and the result is shown in Fig. 4. It can be seen that the static thrust of the aircraft is approximately 4 N. As the advance ratio is varied, the thrust eventually becomes negative. This means that such high advance ratios can only be maintained during dive and not in sustained flight. Overall, the thrust varies with the advance ratio in a parabolic fashion, which is in close agreement to Null *et al.* (2005). The purpose of this mapping was to evaluate the dynamic thrust data as a function of advance ratio and angle of attack. In order to get true aerodynamic coefficients, the dynamic thrust values need to be subtracted from lift and drag data as shown in Eq. 2. It should be noted that D_{prop} is negative and represents the propeller thrust.

$$L_{aero} = L_{total} - L_{prop}$$
$$D_{aero} = D_{total} + D_{prop} \quad (2)$$

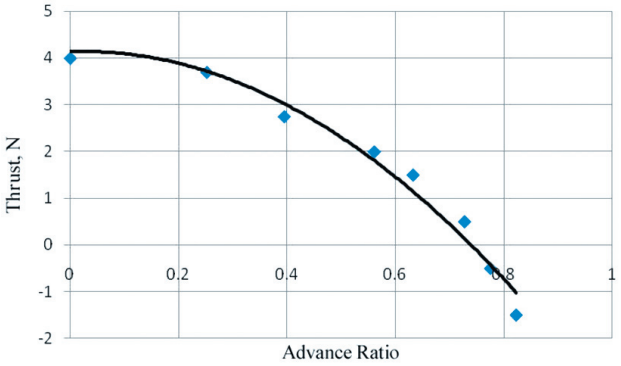

Figure 4. Thrust variation with the change in the advance ratio.

RESULTS AND DISCUSSION

In this section, the results from powered testing are discussed. As mentioned earlier, the study was restricted to longitudinal plane and the effect of swirl on the lateral-directional forces and moments was out of the scope of the study. The minor variations in powered data can be attributed to the propeller rotation, whether the wings are behind an upward or downward moving blade. The resultant aerodynamic characteristics on both sides of the fuselage will differ slightly. The trend for the coefficient of lift across angles of attack and various advance ratios is plotted in Fig. 5. The coefficient of lift (C_L) variation at zero angle of attack for various advance ratios was seen. Specifically, C_L varies from

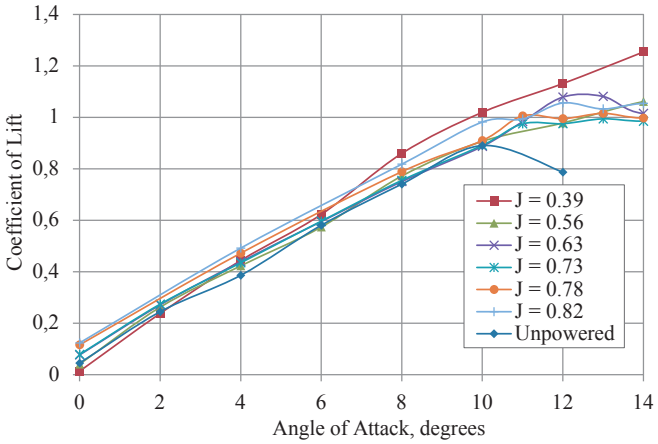

Figure 5. Coefficient of lift behavior with the variation in angle of attack and advance ratio.

-0.04 for unpowered case to 0.1 for high advance ratio. The zero lift angle of attack becomes negative with the increase in advance ratio. This observation is consistent with the investigations carried out by Witkowski *et al.* (1989a). The lift curve slope seems to follow linear tendency for advance ratio varying from 0.39 to 0.82. The decrease in lift-curve slope was observed with the increase in advance ratio. However, the variation was very small (less than 1%) and thus can be neglected for simplification. Witkowski *et al.* (1989a) have observed a decrease in lift-curve slope of 3.5% with the increase in advance ratio. The investigations by Null *et al.* (2005) show that the variation of lift-slope diminishes between powered and unpowered cases as the camber is increased. The airfoil used in this experiment is not cambered but has a thickness-to-chord ratio of 12%. The small difference in the lift-curve slope variation in the current experiment might be caused by the thickness of the airfoil and not by the camber. However, confirmation on this fact still needs further investigations. The coefficient of lift (C_L) is shown up to a 14° angle of attack (Fig. 5), in order that the C_L behavior can be observed clearly and the stall pattern will be discussed separately.

The power-induced flow affects significantly the stall angle of attack, which is, generally, different for both wings. The wing facing upward moving blade stalls slightly earlier whereas the downward moving blade side experience slightly delayed stall. Overall, the stall angle of attack will be delayed on both sides relative to unpowered case because the prop-stream energizes the flow around the affected part of the wing. The stall angle of attack over here is taken as a cumulative effect and recorded against the first dip in the coefficient of lift curve. The trend for stall angle of attack for several advance ratios is shown in Fig. 6.

It is remarkable that the stall angle of attack in powered scenarios can be expressed in inverse-quadratic relationship with advance ratio. Equation 3 shows the generic power law model used to fit the stall angle of attack behavior with respect to advance ratio:

$$\alpha_{stall,p} = \frac{a}{J^2} + \alpha_{stall,up} \quad (3)$$

where for our case:
$\alpha_{stall,p}$: stall angle of attack for powered case,
$\alpha_{stall,up}$: stall angle of attack for unpowered case,
α = 1.5, $\alpha_{stall,up}$ = 9.6 and $\alpha_{(.)}$: in degrees.

The coefficient of determination, R^2 value of the power law fit is 0.9791, which ensures its adequacy. For high *d/b* values, where most area of the wing is under prop-stream, this relationship governs the overall shift in the stall behavior specific to the current scenario. For low-advance ratios, the prop-stream will not let the aircraft stall even at very high angles of attack, since the high energy is imparted to low-energy flow field. However, as the advance ratio is increased, the stall angle will approach the unpowered/windmill case. The difference between the settling stall angle of attack from the quadratic fit and experimental data is 0.4º, which is negligible for practical purposes.

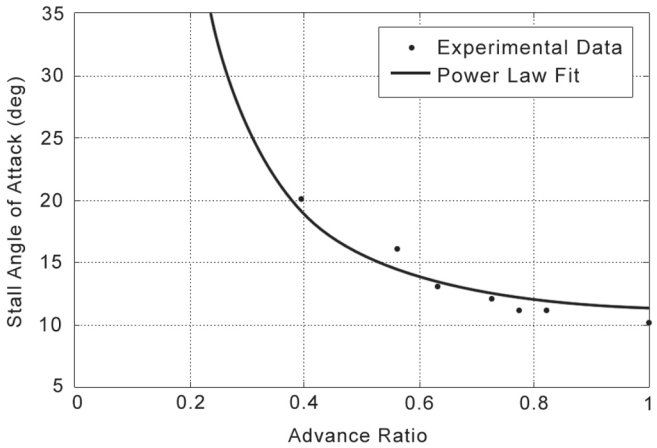

Figure 6. Stall angle of attack variation with advance ratio.

CONCLUSIONS

Propeller-induced flow-field has a significant impact on the aerodynamic characteristics of small UAV/micro air vehicle (MAV) specifically for high *d/b* values. The effects are more pronounced as the advance ratio is decreased (high power flight). The powered test shows functional independence of the magnitude of lift-curve slope against advance ratios. However, stall angle of attack has a strong functional dependence against the advance ratio, and such dependence can be modeled accurately using inverse-quadratic relationship. This empirical trend of the stall behavior with advance ratio might be useful in the analysis and simulation of the resulting flight. Moreover, the study indicates the need for a unified theory on the stall angle dependence with *d/b* and advance ratios, which can be very useful during early aircraft design stage.

REFERENCES

Barlow, J. B. *et al.*, 1999, "Low-speed wind tunnel testing", Michigan University, Wiley.

Frank, A. *et al.*, 2007, "Hover, Transition, and Level Flight Control Design for a Single-Propeller Indoor Airplane", In: AIAA Guidance, Navigation and Control Conference and Exhibit, South Carolina, USA.

Green, W.E. and Oh, P.Y., 2005, "A MAV That Flies Like an Airplane and Hovers Like a Helicopter", In: IEEE International Conference on Advanced Intelligent Mechatronics, Monterey, California.

Maqsood, A. and Go, T.H., 2010, "Optimization of Hover-to-Cruise Transition Maneuver Using Variable-Incidence Wing", Journal of Aircraft, Vol. 47, No. 3, pp. 1060-1064.

Null, W. *et al.*, 2005, "Effects of Propulsive-Induced Flow on the Aerodynamic of Micro Air Vehicles", In: 23rd AIAA Applied Aerodynamics Conference, Toronto, Ontario, Canada.

Ralston, J. and Hultberg, R., 2010, "Full-Envelope Aerodynamics Modeling of a General Aviation Aircraft with Propeller Slipstream Effects", In: AIAA Modeling and Simulation Technologies Conference, Toronto, Ontario, Canada.

Stone, H., 2002, "Aerodynamic Modelling of a Wing-in-Slipstream Tail-Sitter UAV", In: 2002 Biennial International Powered Lift Conference and Exhibit, Williamsburg, Virginia.

Stone, H. *et al.*, 2008, "Flight Testing of the T-Wing Tail-Sitter Unmanned Air Vehicle", Journal of Aircraft, Vol. 45, No. 2, pp. 673-685.

Taylor, D.J. and Thomas Cord, M.V.O., 2003, "SkyTote: an unmanned precision cargo delievery system", In: AIAA/ICAS International Air and Space Symposium and Exposition, The Next 100 Y, Dayton, Ohio.

Witkowski, D.P. *et al.*, 1989a, "Propeller/Wing Interaction", In: 27th Aerospace Sciences Meeting, Reno, Nevada.

Witkowski, D.P. *et al.*, 1989b, "Aerodynamic Interaction Between Propellers and Wings", Journal of Aircraft, Vol. 26, No. 9, pp. 829-836.